Effect of Cation on Dye Regeneration Kinetics of N719-sensitized TiO_2 Films in Acetonitrile-based and Ionic-Liquid-based Electrolytes Investigated by Scanning Electrochemical Microscopy

Supporting Information

Ushula Mengesha Tefashe,[a] Kazuteru Nonomura,[b] Nikolaos Vlachopoulos,[b] Anders Hagfeldt,[b] Gunther Wittstock[a]*

[a] Ushula Mengesha Tefashe, Prof. Dr. Gunther Wittstock
Department of Pure and Applied Chemistry, Center of Interface Science, Faculty of Mathematics and Natural Sciences, Carl von Ossietzky University of Oldenburg, D-26111 Oldenburg, Germany

[b] Dr. Kazuteru Nonomura, Dr. Dr. Nikolaos Vlachopoulos, Prof. Dr. Anders Hagfeldt
Department of Physical and Analytical Chemistry, Physical Chemistry, Uppsala University, S-75105 Uppsala, Sweden

* To whom correspondence should be addressed
phone, (+49-441) 798 3971, fax (+49-441) 798 3979
e-mail: gunther.wittstock@uni-oldenburg.de

SI 1. Schematics of SECM experimental set-up for DSSC

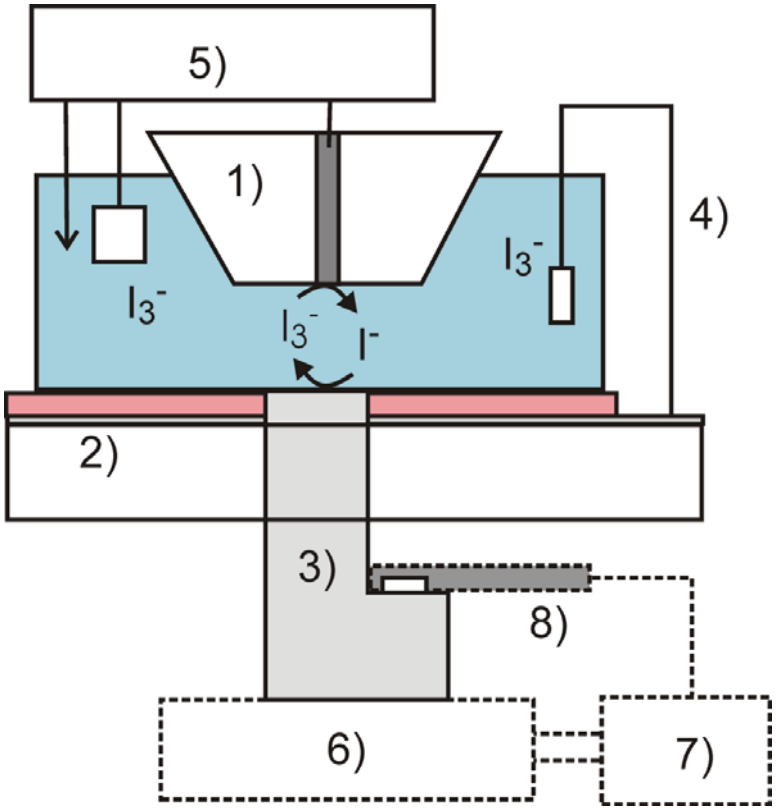

Figure SI-1 Schematic of SECM setup to investigate redox processes at a DSSC. 1) UME, 2) F-doped glass with coating of dye-sensitized film, 3) illumination path, 4) short contact of the DSSC by a Pt wire, 5) potentiostat with UME as working electrode and reference and counter electrode. In case of intensity dependent measurement (dashed lines) a regulated LED light source (6) was powered with a potentiostat (7). The intensity was measured by a light sensor (8) and fed back to the power potentiostat (7).

SI 2. Fitting of steady-state SECM approach curves with finite first order kinetics at the sample and diffusion controlled kinetics at the UME

Normalized heterogeneous rate constants κ have been extracted from experimental approach curves by fitting them to an analytical approximation of simulated data evaluated by Cornut and Lefrou.[1] The radius of the active part of the UME, r_T, the ratio RG of insulating sheath r_{glass} and r_T, and the point of closest approach d_0 have been determined from independent experiments. *RG* was determined by optical microscopy; r_T and d_0 were determined from approach curves to glass or N719/TiO_2 film in the dark and fitting them to theoretical curves proposed by Amphlett and Denuault.[2] Normalized approach curves I_T vs. L have been calculated from experimental approach curves $i_T(z)$ using equation (SI-1) and equation (SI-2). Equation (SI-2) applies for increasing motor position z for decreasing UME-to-sample distance d (Figure SI-2).

$$I_T = \frac{i_T}{i_{T,\infty}} \qquad \text{(SI-1)}$$

$$L = \frac{z - z_{offset}}{-r_T} \qquad \text{(SI-2)}$$

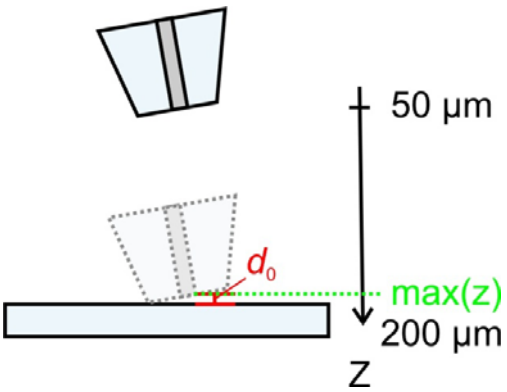

Figure SI-2 Determination of z_{offset} and L for increasing z for decreasing d

z_{offset} is calculated according to equation (SI-3):

$$z_{offset} = \max(z) + d_0 \qquad \text{(SI-3)}$$

The analytical approximation of Cornut and Lefrou[1] was used for calculating a theoretical current I_T for each experimental, normalized distance L.

$$I_T(L,\kappa,RG) = I_T^{\,\mathrm{cond}}\left(L+\frac{1}{\kappa},RG\right) + \frac{I_T^{\,\mathrm{ins}}(L,RG)-1}{\left(1+2.47RG^{0.31}L\kappa\right)\left(1+L^{0.006RG+0.113}\kappa^{-0.0236RG+0.91}\right)} \quad \text{(SI-4)}$$

with

$$I_T^{\,\mathrm{cond}}\left(L+\frac{1}{\kappa},RG\right) = \alpha(RG) + \frac{1}{2\beta(RG)\xi\left(L+\frac{1}{\kappa}\right)} + \left(1-\alpha(RG)-\frac{1}{2\beta(RG)}\right)\xi\left(L+\frac{1}{\kappa}\right) \quad \text{(SI-5)}$$

$$I_T^{\,\mathrm{ins}}(L,RG) = \frac{\frac{2.08}{RG^{0.358}}\left(L-\frac{0.145}{RG}\right)+1.585}{\frac{2.08}{RG^{0.358}}(L+0.0023RG)+1.57+\frac{\ln RG}{L}+\frac{2}{\pi RG}\ln\left(1+\frac{\pi RG}{2L}\right)} \quad \text{(SI-6)}$$

$$\alpha(RG) = \ln 2 + \ln 2\left(1-\frac{2}{\pi}\arccos\left(\frac{1}{RG}\right)\right) - \ln 2\left(1-\left(\frac{2}{\pi}\arccos\left(\frac{1}{RG}\right)\right)^2\right) \quad \text{(SI-7)}$$

$$\beta(RG) = 1 + 0.639\left(1-\frac{2}{\pi}\arccos\left(\frac{1}{RG}\right)\right) - 0.186\left(1-\left(\frac{2}{\pi}\arccos\left(\frac{1}{RG}\right)\right)^2\right) \quad \text{(SI-8)}$$

$$\xi\left(L+\frac{1}{\kappa}\right) = \frac{2}{\pi}\arctan\left(L+\frac{1}{\kappa}\right) \quad \text{(SI-9)}$$

$$\kappa = \frac{k_{\mathrm{eff}}\,r_T}{D} \quad \text{(SI-10)}$$

κ, $i_{T,\infty}$ and d_0 (within reasonable range) were varied in order to fit the experimental approach curves.

SI 3. Determining diffusion coefficient of I_3^- in RTILs with various concentration of supporting electrolytes

Figure SI-3 shows cyclic voltammograms for the redox reaction of I_3^- at Pt UME (r_T =12.5 μm) in the electrolyte composed of 0.95 mM LiI, 0.95 mM I_2 and 0.01–2.55 M LiTFS in EMimTFS, measured at a scan rate of 50 mV s^{-1}. The voltammograms show a two sigmodal waves, corresponding to the reduction and oxidation of I_3^- to I^- and I_2, respectively. Like in acetonitrile solution, the ratio of cathodic and anodic wave heights is approximately 2/3 and the plateau at E = 0.05 V lies on zero current regime, confirming that equimolar amounts of I^- and I_2 were mixed, which yields I_3^- as the only relevant redox active species in the electrolyte.[3] The steady-state reduction currents for I_3^- gradually decreased as the concentration of inert supporting electrolyte increases, while the steady-state oxidation currents did not change. It should be noted that higher inert supporting electrolyte concentration is expected to yield higher viscosity of the electrolyte. Accordingly, it is considered that this property reduces the mobility of ions and hence the steady-state currents at the UME tip. When the steady state condition is obtained, the diffusion coefficients D of tri-iodide in different electrolytes concentration could be determined from diffusion-limited UME tip-currents using the following equation:

$$D = \frac{i_{T,\infty}}{8FD[I_3^-]^* r_T} \qquad \text{(SI-11)}$$

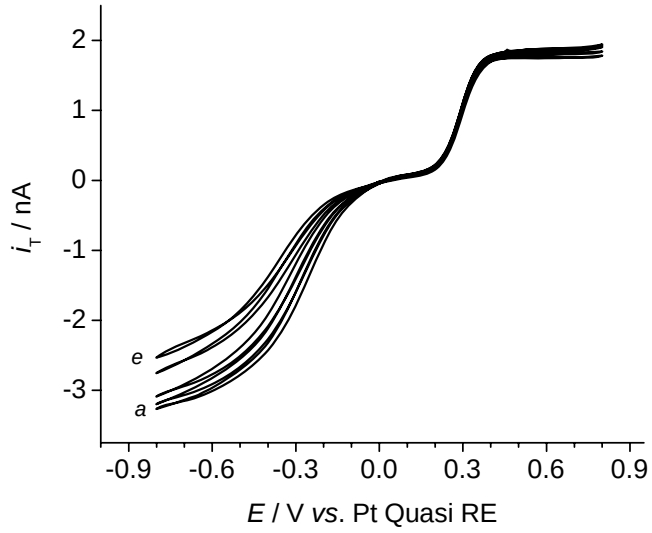

Figure SI-3 Typical cyclic voltammograms obtained at a Pt disk UME (r_T = 12.5 µm) in 0.95 mM I_3^-. The concentration of LiTFS from *a* to *e* are 0.02 M, 0.5 M, 1.05 M, 2.02 M and 2.5 M, respectively.

Table SI-1: Tri-iodide diffusion coefficients for the systems LiI/I_2/LiTFS, $DMPimI/I_2$/DMPimTFS and $TBAI/I_2$/TBATFS in EMimTFS with 0.95 mM $[I_3^-]^*$ and varying supporting electrolyte concentration ranging from 0.01 to 2.5 M.

Concentration of added supporting electrolyte [M]	D / 10^{-7} cm^2 s^{-1}		
	LiI/I_2/LiTFS	$DMPimI/I_2$/DMPimTFS	$TBAI/I_2$/TBATFS
0.01	8.10	7.36	2.26
0.5	6.27	5.45	1.09
1.05	5.18	4.64	1.03
1.51	4.36	4.17	1.01
2.02	3.82	3.08	0.99
2.5	2.90	2.45	0.90

SI 4. Summary of k_{eff} for dye regeneration reaction in acetonitrile and EMimTFS

Table SI-2. Apparent heterogeneous first-order rate constants k_{eff} derived from normalized apparent heterogeneous first order rate constants κ for the reduction of photoexcited N719 by I^- in acetonitrile and in EMimTFS. $D(I_3^-)$is 1.37×10^{-5} cm^2 s^{-1} in acetonitrile, and 7.31×10^{-7} cm^2 s^{-1} (

Table SI-1) in EMimTFS, r_T = 12.5 µm, RG = 10, $k_{eff} = \kappa D/r_T$

(a) For varying $[I_3^-]^*$ at a fixed LED illumination intensity, $J_{hv} = 25.5 \times 10^{-9}$ mol cm^{-2} s^{-1}

$[I_3^-]^*$ / 10^{-6} mol cm^{-3}	k_{eff} / 10^{-3} cm s^{-1}	
	acetonitrile	EMimTFSI
0.064	19.73	0.336
0.136	13.37	0.201
0.622	8.22	0.104
0.953	3.51	0.1
1.24	1.86	0.052
2.21	0.658	0.025

(b) For varying LED illumination intensity at fixed $[I_3^-]^*$ = 0.064 mol cm^{-3}

J_{hv} / 10^{-9} mol cm^{-2} s^{-1}	k_{eff} / 10^{-3} cm s^{-1}	
	acetonitrile	EMimTFS
0.982	0.464	0.0053
1.7	2.87	0.0246
4.5	5.82	0.114
9.1	8.83	0.269
15.1	15.2	0.316
25.5	19.9	0.392

SI 5. Complete derivation of SECM model for dye regeneration

The following reaction mechanism for dye regeneration is widely accepted and we develop a model for steady state SECM experiments in the feedback mode.

$$D/TiO_2 + h\nu \xrightarrow{\phi_{h\nu}} D^*/TiO_2 \quad \text{(SI-12)}$$

$$D^*/TiO_2 \xrightarrow{k_{inj}} D^+/TiO_2 + e^-_{CB}(TiO_2) \quad \text{(SI-13)}$$

$$D^+/TiO_2 + I^- \xrightarrow{k_1} [D\cdots I]/TiO_2 \quad \text{(SI-14)}$$

$$[D\cdots I]/TiO_2 + I^- \xrightarrow{k_2} D/TiO_2 + I_2^{-\bullet} \quad \text{(SI-15)}$$

$$2\, I_2^{-\bullet} \xrightarrow{k_3} I_3^- + I^- \quad \text{(SI-16)}$$

Steady state for $[D^*]$

$$\frac{\partial\left[D^*\right]}{\partial t} = 0 = \phi_{h\nu} J_{h\nu}\left[D\right] - k_{inj}\left[D^*\right] \quad \text{(SI-17)}$$

$$\frac{\left[D\right]}{\left[D^*\right]} = \frac{k_{inj}}{\phi_{h\nu} J_{h\nu}} \quad \text{(SI-18)}$$

Steady state for $[D\cdots I]$

$$\begin{aligned}\frac{\partial\left[D\cdots I\right]}{\partial t} = 0 &= k_1\left[D^+\right]\left[I^-\right]_S - k_2\left[D\cdots I\right]\left[I^-\right]_S \\ &= k_1\left[D^+\right] - k_2\left[D\cdots I\right]\end{aligned} \quad \text{(SI-19)}$$

$$\frac{\left[D\cdots I\right]}{\left[D^+\right]} = \frac{k_1}{k_2} \quad \text{(SI-20)}$$

Diffusion limited tip current (n = 2) for reduction of one I_3^-

$$i_{\mathrm{T,lim}} = 8FD\left[\mathrm{I_3^-}\right]^{*} r_{\mathrm{T}} I_{\mathrm{T}}(L) \tag{SI-21}$$

Steady state for $[D^+]$

$$\frac{\partial\left[\mathrm{D^+}\right]}{\partial t} = 0 = k_{\mathrm{inj}}\left[\mathrm{D^*}\right] - k_1\left[\mathrm{D^+}\right]\left[\mathrm{I^-}\right]_{\mathrm{S}} \tag{SI-22}$$

$$\frac{\left[\mathrm{D^+}\right]}{\left[\mathrm{D^*}\right]} = \frac{k_{\mathrm{inj}}}{k_1\left[\mathrm{I^-}\right]_{\mathrm{S}}} \tag{SI-23}$$

Combining (SI-20) with (SI-23)

$$\frac{\left[\mathrm{D\cdots I}\right]}{\left[\mathrm{D^*}\right]} = \frac{k_{\mathrm{inj}}}{k_2\left[\mathrm{I^-}\right]_{\mathrm{S}}}$$

Mass balance for the total dye content

$$\begin{aligned}\left[\mathrm{D^0}\right] &= \left[\mathrm{D}\right] + \left[\mathrm{D^+}\right] + \left[\mathrm{D^*}\right] + \left[\mathrm{D\cdots I}\right] \\ &= \left[\mathrm{D^*}\right]\left(\frac{\left[\mathrm{D}\right]}{\left[\mathrm{D^*}\right]} + \frac{\left[\mathrm{D^+}\right]}{\left[\mathrm{D^*}\right]} + \frac{\left[\mathrm{D\cdots I}\right]}{\left[\mathrm{D^*}\right]} + 1\right)\end{aligned} \tag{SI-24}$$

Steady state expression for ratio of $[D^0]$

$$\left[\mathrm{D^0}\right] = \left[\mathrm{D^*}\right]\left(\frac{k_{\mathrm{inj}}}{\phi_{h\nu} J_{h\nu}} + \frac{k_{\mathrm{inj}}}{k_1\left[\mathrm{I^-}\right]_{\mathrm{S}}} + \frac{k_{\mathrm{inj}}}{k_2\left[\mathrm{I^-}\right]_{\mathrm{S}}} + 1\right) \tag{SI-25}$$

$$\left[\mathrm{D^*}\right] = \frac{\left[\mathrm{D^0}\right]}{\frac{k_{\mathrm{inj}}}{\phi_{h\nu} J_{h\nu}} + \frac{k_{\mathrm{inj}}}{k_1\left[\mathrm{I^-}\right]_{\mathrm{S}}} + \frac{k_{\mathrm{inj}}}{k_2\left[\mathrm{I^-}\right]_{\mathrm{S}}} + 1} \tag{SI-26}$$

Expression for current, i_k ($[I^-]_s$ is the iodide concentration at the surface of the dye-sensitized electrode)

$$i_K = nFA\left(k_1 l[D^+][I^-]_S\right), \quad \text{(SI-27)}$$

Substitution of the bracketed term using the Bodenstein principle for the steady state experiment (SI-22) $k_{inj}[D^*] = k_1 l[D^+][I^-]_S$ (n = 1)

$$i_K = FAk_{inj} l[D^*] \quad \text{(SI-28)}$$

Substitute the expression for $[D^*]$ from mass balance (SI-26).

$$i_K = FAk_{inj} l \frac{[D°]}{\frac{k_{inj}}{\phi_{h\nu} J_{h\nu}} + \frac{k_{inj}}{k_1[I^-]_S} + \frac{k_{inj}}{k_2[I^-]_S} + 1} \quad \text{(SI-29)}$$

$$i_K = FAl\left[D^0\right] \frac{\phi_{h\nu} J_{h\nu} k_1 k_2 \left[I^-\right]_S k_{inj}}{k_1 k_2 \left[I^-\right]_S k_{inj} + k_{inj}\phi_{h\nu} J_{h\nu} k_2 + k_{inj}\phi_{h\nu} J_{h\nu} k_1 + k_1 k_2 \phi_{h\nu} J_{h\nu} \left[I^-\right]_S} \quad \text{(SI-30)}$$

$$\frac{1}{i_K} = \frac{1}{FAl[D°]\phi_{h\nu} J_{h\nu}} + \frac{1}{FAl[D°]k_1[I^-]_S} + \frac{1}{FAl[D°]k_2[I^-]_S} + \frac{1}{FAl[D°]k_{inj}} \quad \text{(SI-31)}$$

Simplifying the expression for light absorption, electron injection and dye regeneration by summarizing the steps using $\left(k_{h\nu,\text{eff}}\right)^{-1} = \left(k_{inj}\right)^{-1} + \left(\phi_{h\nu} J_{h\nu}\right)^{-1} \approx \left(\phi_{h\nu} J_{h\nu}\right)^{-1}$ and $\left(k_{ox}^{'}\right)^{-1} = \left(k_1\right)^{-1} + \left(k_2\right)^{-1}$

$$\frac{1}{i_K} = \frac{1}{FAl[D°]k_{h\nu,\text{eff}}} + \frac{1}{FAl[D°]k_{ox}^{'}[I^-]_S} \quad \text{(SI-32)}$$

The limiting substrate current would be reached if the iodide concentration is 3 time the triiodide concentration, i.e. all iodide formed at the tip is available to the sample without any dilution, $[I^-]_S = 3[I_3^-]^*$

$$\frac{1}{i_{\mathrm{K,lim}}} = \frac{1}{FAl[\mathrm{D}^\circ]k_{h\nu,\mathrm{eff}}} + \frac{1}{3FAl[\mathrm{D}^\circ]k_{\mathrm{ox}}^{'}[\mathrm{I}_3^-]^*} \tag{SI-33}$$

Normalizing the limiting substrate by $i_{\mathrm{T},\infty}$ yields $I_{\mathrm{K,lim}}$

$$I_{\mathrm{K,lim}} = \frac{i_{\mathrm{K,lim}}}{i_{\mathrm{T},\infty}} = \frac{i_{\mathrm{K,lim}}}{4nFD[\mathrm{I}_3^-]^* r_{\mathrm{T}}},\ n = 2 \text{ at the tip for } \mathrm{I}_3^-,\ A \approx \pi {r_{\mathrm{T}}}^2 \tag{SI-34}$$

$$\frac{1}{I_{\mathrm{S}}} = \frac{i_{\mathrm{T},\infty}}{i_{\mathrm{K,lim}}} + \frac{1}{I_{\mathrm{T,cond}}} + \frac{1}{I_{\mathrm{el,lim}}},\ \frac{1}{I_{\mathrm{el,lim}}} \approx 0 \tag{SI-35}$$

$$\begin{aligned} \frac{1}{I_{\mathrm{S}}} &= \frac{1}{I_{\mathrm{T,cond}}} + \frac{8FD[\mathrm{I}_3^-]^* r_{\mathrm{T}}}{F\pi r_{\mathrm{T}}^2 l[\mathrm{D}^\circ]\phi_{h\nu} J_{h\nu}} + \frac{8FD[\mathrm{I}_3^-]^* r_{\mathrm{T}}}{3F\pi r_{\mathrm{T}}^2 l[\mathrm{D}^\circ]k_{\mathrm{ox}}^{'}[\mathrm{I}_3^-]^*} \\ &= \frac{1}{I_{\mathrm{T,cond}}} + \frac{8D[\mathrm{I}_3^-]^*}{\pi r_{\mathrm{T}} l[\mathrm{D}^\circ]\phi_{h\nu} J_{h\nu}} + \frac{8D}{3\pi r_{\mathrm{T}} l[\mathrm{D}^\circ]k_{\mathrm{ox}}^{'}} \end{aligned} \tag{SI-36}$$

Comparison to uncomplicated first order process at the sample[4]

$$\begin{aligned} &\frac{1}{I_{\mathrm{S}}} = \frac{1}{I_{\mathrm{T,cond}}} + \frac{4}{\pi}\frac{1}{\kappa},\quad \kappa = k_{\mathrm{eff}}\frac{r_{\mathrm{T}}}{D} \\ &\frac{1}{I_{\mathrm{S}}} = \frac{1}{I_{\mathrm{T,cond}}} + \frac{4D}{\pi r_{\mathrm{T}}}\frac{1}{k_{\mathrm{eff}}} \end{aligned} \tag{SI-37}$$

$$\frac{1}{I_{\mathrm{S}}} = \frac{1}{I_{\mathrm{T,cond}}} + \frac{4D}{\pi r_{\mathrm{T}}}\left[\frac{2[\mathrm{I}_3^-]^*}{l[\mathrm{D}^\circ]\phi_{h\nu} J_{h\nu}} + \frac{2}{3l[\mathrm{D}^\circ]k_{\mathrm{ox}}^{'}}\right] \tag{SI-38}$$

$$\frac{1}{k_{\mathrm{eff}}} = \frac{2[\mathrm{I}_3^-]^*}{l[\mathrm{D}^\circ]\phi_{h\nu} J_{h\nu}} + \frac{2}{3l[\mathrm{D}^\circ]k_{ox}^{'}} \tag{SI-39}$$

$$k_{\mathrm{eff}} = \frac{3l[\mathrm{D}^0]\phi_{h\nu} J_{h\nu} k_{ox}^{'}}{6k_{\mathrm{ox}}^{'}[\mathrm{I}_3^-]^* + 2\phi_{h\nu} J_{h\nu}} \tag{SI-40}$$

SI 6. SECM approach curves on N719/TiO_2 film for the solution compositions of (a) DMPimI/I_2/DMPimTFS and (b) TBAI/I_2/TBATFS in EMimTFS

(a) (b)

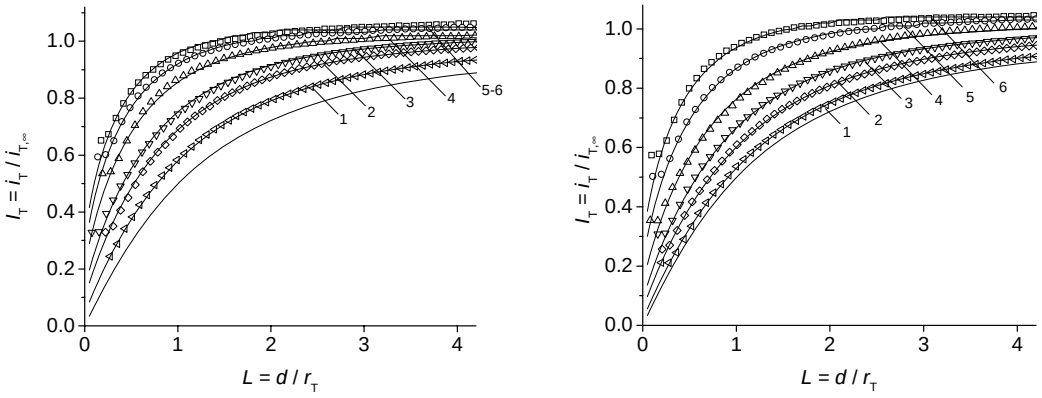

Figure SI-4. Normalized SECM approach curves with Pt UME (r_T = 12.5 μm) on TiO_2/N719 film illuminated with green LED (J_{hv} = 25.5 × 10^{-9} mol cm^{-2} s^{-1}) and $[I_3^-]^*$ = 0.064 mM at various concentration of (a) DMPimTFS and (b) TBATFS in EMimTFS, respectively: (1) 2.5 M, (2) 2.02 M, (3) 1.51 M, (4) 1.05 M, (5) 0.5 M, and (6) 0.02. The summary of κ value obtained from the best fit of experimental approach curves (open symbols) to the theoretical model[1] (thin solid curves), respectively, (a) (1) 0.019, (2) 0.06, (3) 0.093, (4) 0.17, (5) 0.24, (6) 0.29 and (b): (1) 0.006, (2) 0.026, (3) 0.05, (4) 0.10, (5) 0.18, (6) 0.26.

Table SI-3. Apparent heterogeneous first-order rate constants k_{eff} derived from normalized apparent first order rate constants κ for the reduction of photo-oxidized N719 by I^- in EMimTFS for the electrolyte compositions LiI/I_2/LiTFS, DMPimI/I_2/DMPimTFS and TBAI/I_2/TBAS with a fixed $[I_3^-]_*$ and varying cations concentration. $D(I_3^-)$ was calculated for each concentration of the inert supporting electrolyte (Table SI-1) r_T = 12.5 µm, RG = 10, $k_{eff} = \kappa D/r_T$

Concentration of added supporting electrolyte [M]	k_{eff} / 10^{-4} cm s^{-1}		
	LiI/I_2/LiTFS	DMPimI/I_2/DMPimTFS	TBAI/I_2/TBAS
0.01	2.24	1.71	0.47
0.5	1.1	1.05	0.16
1.05	0.54	0.63	0.082
1.51	0.22	0.31	0.040
2.02	0.0092	0.15	0.021
2.5	2.3×10^{-4}	0.0037	4.3×10^{-3}

SI 7. SECM approach curves on N719/TiO_2 film for different concentration of LiTFS, DMPimTFS and TBAS in acteonitrile with 0.064 mM [I_3^-]*

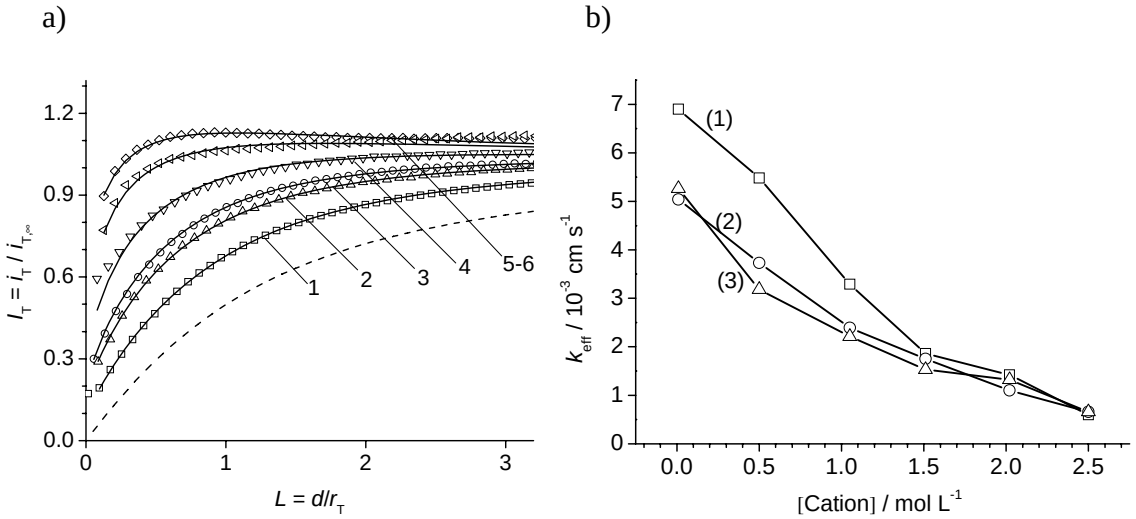

Figure SI-5 (a) Normalized SECM approach curves on TiO_2/N719 film at the same conditions as in Figure SI-4 for various concentrations of LiTFS in acetonitrile. [LiTFS]: (1) 2.5 M, (2) 2.02 M, (3) 1.51 M, (4) 1.05 M, (5) 0.5 M, and (6) 0.01. The summary of κ values from the best fit to the theoretical model[1] were, κ = (1) 0.055, (2) 0.13, (3) 0.17, (4) 0.3, (5) 0.5, and (6) 0.63, respectively. (b) Plot of k_{eff} as a function of cation concentration for three different electrolytes compositions in acetonitrile varying only in terms of cation counter ions (1) LiI/I_2/LiTFS, (2) DMPimI/I_2/DMPimTFS, (3) TBAI/I_2/TBATFS in EMimTFS. Lines are guides to the eye.

Table SI-4. Apparent heterogeneous first-order rate constants k_{eff} derived from normalized apparent first order rate constants κ for the reduction of photo-oxidized N719 by I^- in acetonitrile for the electrolyte compositions LiI/I_2/LiTFS, DMPimI/I_2/DMPimTFS and TBAI/I_2/TBAS with a fixed $[I_3^-]_*$ and varying cations concentration. $D(I_3^-)$ was calculated for each concentration of the inert supporting electrolyte (Table SI-1) r_T = 12.5 µm, RG = 10, $k_{eff} = \kappa D/r_T$

Concentration of added supporting electrolyte [M]	k_{eff} / 10^{-3} cm s^{-1}		
	LiI/I_2/LiTFS	DMPimI/I_2/DMPimTFS	TBAI/I_2/TBAS
0.01	6.9	5.04	5.26
0.5	5.48	3.73	3.18
1.05	3.29	2.39	2.21
1.51	1.86	1.75	1.53
2.02	1.42	1.1	1.32
2.5	0.60	0.66	0.66

References

(1) Cornut, R.; Lefrou, C. *J. Electroanal. Chem.* **2008**, *621*, 178-184.
(2) Amphlett, J. L.; Denuault, G. *J. Phys. Chem. B* **1998**, *102*, 9946-9951.
(3) Macagno, V. A.; Giordano, M. C. *Electrochim. Acta* **1969**, *14*, 335-357.
(4) Wei, C.; Bard, A. J.; Mirkin, M. V. *J. Phys. Chem.* **1995**, *99*, 16033-16042.